Available online at www.sciencedirect.com

ScienceDirect

Ceramics International 40 (2014) 811–820

CERAMICS INTERNATIONAL

www.elsevier.com/locate/ceramint

Influence of the chemical and mineralogical composition on the reactivity of volcanic ashes during alkali activation

Patrick N. Lemougna[a,*], U.F. Chinje Melo[a], Marie-Paule Delplancke[b], Hubert Rahier[c]

[a]*Physico-Chemistry of Mineral Materials Laboratory, University of Yaoundé I, and Local Materials Promotion Authority, MINRESI/MIPROMALO, P.O. Box 2396, Yaoundé, Cameroon*

[b]*4MAT, Université libre de Bruxelles, avenue Roosevelt 50, CP 165/63, 1050 Brussels, Belgium*

[c]*Department of Materials and Chemistry, Vrije Universiteit Brussel, Pleinlaan 2, 1050 Brussels, Belgium*

Received 21 May 2013; received in revised form 19 June 2013; accepted 19 June 2013
Available online 2 July 2013

Abstract

The influence of chemical and mineralogical compositions on alkali activation of four natural volcanic ashes was investigated. NaOH was used as the sole alkaline activator. The reactivity of the systems was studied with Differential Scanning Calorimetry. The X-ray spectra of reacted materials showed a mixture of amorphous and crystalline phases. The SEM micrographs showed that the dissolution of larger particles is incomplete while smaller particles dissolved in the activating solution forming the glassy aluminosilicate matrix. The infrared spectra showed a broad absorbance at 820–1250 $cm^{-1}$and 480–600 cm^{-1} assigned to internal vibration of Si–O–Si and Si–O–Al in both raw volcanic ash and resulting inorganic polymers. The reactivity of the volcanic ashes was found to correlate with their amorphous fraction. The dry compressive strength of synthesized products from all the ashes were in the range 14–63 MPa, suggesting their possible utilization as building materials. However, the strength was found to decrease (1–28 MPa) after specimens' immersion overnight in water, but was partly or totally recovered after overnight drying at 90 °C.

Keywords: C. Mechanical properties; C. Thermal properties; D. Silicate; E. Structural applications

1. Introduction

Volcanic ashes are vitreous pyroclastic materials produced by violent eruptive volcanic action [1]. During volcanic eruptions, particularly of the Strombolian-type, pozzolans are ejected on the surface of the earth, forming layers several meters thick. Throughout the world there are volcanoes (eg. Mount St. Helens in the USA., Etna in Italy, Pinatubo in the Philippines, Tarawera in New Zealand, Santiaguito and Pacaya in Guatemala, Fuego in Costa Rica) which have produced huge quantities of pozzolans [2]. In Cameroon, most volcanic eruptions over millions of years in the tertiary period were accompanied by the ejection of pozzolans. Consequently, many cones of volcanic ash exist along the 'Cameroon line' oriented N30°E, specially at the side of mount Cameroon, mount Maneguba, the Tombel plain around Djoungo, the Noun plain around Foumbot, the Kumba plain, the region of lake Nyos and the Adamaoua plateau. The latest eruption of mount Cameroon in 1999, as with previous eruptions, resulted in millions of tones of volcanic materials covering vast areas with mineral deposits [2,3]. Due to their rich content in alumina and silica, volcanic ashes have been found to be possibly suitable for alkali activation to produce construction materials [4,5].

Alkali activation involves mechanisms such as dissolution of aluminosilicates (amorphous or semi crystalline) in a strongly basic medium, followed by polymerization of surface active groups of particles with the dissolved species to form a solid structure [6–9]. Starting from fly ash or metakaolinite geopolymers are formed [1]. The later consists of chain and three dimensional networks made of various Q units of connected SiO_4 and AlO_4 tetrahedra [9–11]. The presence of alkaline ions such as Na^+, K^+, Li^+ in the network is necessary to compensate the negative charge of Al^{3+} in IV-fold coordination [8,9]. In the text the

*Corresponding author. Tel.: +237 22 22 94 45; fax: +237 22 22 37 20.
E-mail address: lemougna@yahoo.fr (P.N. Lemougna).

0272-8842/$ - see front matter © 2013 Elsevier Ltd and Techna Group S.r.l. All rights reserved.
http://dx.doi.org/10.1016/j.ceramint.2013.06.072

term 'geopolymer' will also be used to denote the materials studied here.

The applications of this technology are wide, including building and refractory materials [1,8–13], and the synthesis process is viewed as environmentally-friendly as limited CO_2 is produced, compared with the OPC manufacturing process [14–20].

Alkali activation of volcanic ashes is however influenced by the difference in mineralogical and chemical composition of the ashes, which may greatly affect the reactivity of the materials as well as the final properties of the synthesized products.

The present study investigates the suitability of four different volcanic ashes from Cameroon for geopolymers synthesis, in order to highlight a possible correlation between the chemical and the mineralogical composition of the ashes and the final properties of the synthesized materials.

NaOH was used as the sole alkaline activator. The reactivity of the systems was studied with Differential Scanning Calorimetry. The resulting products were characterized by Scanning electron microscopy (SEM), Infrared spectroscopy (IR), X-ray diffraction (XRD), Differential Thermal Analysis and Thermogravimetry Analysis (DTA/TGA). The products stability was assessed by dry, wet and wet-dry compressive strength measurements.

2. Experimental

The four volcanic ashes (Va1, Va2, Va3, Va4) used in this study were from Cameroon (the two firsts from Foumbot and rest from Djoungo sites), situated respectively in the west and littoral Regions of Cameroon. The materials were ground to minus 400 μm. Their chemical composition determined by X-ray fluorescence and their particles size distribution determined by sieving–sedimentation are presented in Table 1 and Fig. 1 respectively. Fig. 1 shows the d_{50} of 28, 40, 120 and 65 μm respectively for Va1, Va2, Va3 and Va4. The sodium hydroxide (pro analysis) used was from Merck.

2.1. Geopolymer synthesis

The inorganic polymer formulations were obtained by adding while stirring volcanic ash into a solution obtained by dissolving NaOH in distilled water, as to obtain in the mixtures a Na_2O/Al_2O_3 molar ratio ranging from 1.00 to 1.75, with 0.25 intervals. This has resulted in four compositions for each of the ashes Va1, Va2, Va3, and Va4. The ratio water/ash was maintained to 0.21 for all the compositions.

The mixed pastes were placed in polyethylene cubic molds (4 × 4 cm), and then vibrated for 5 min to remove air bubbles. The molded samples were then placed at 40 °C for 2 days, then, the samples were unmolded and placed at 90 °C for 5 days.

2.2. DSC measurement

Differential scanning calorimetry (isothermal and non-isothermal measurement) was performed on a DSC 822^e

Table 1
Chemical composition (%) of the different ashes.

Oxide	Fe_2O_3	MnO	TiO_2	CaO	K_2O	P_2O_5	SiO_2	Al_2O_3	MgO	Na_2O	SUM
Va1	12	0.19	2.9	11	1.7	0.9	43	15	6.8	4.6	99.39
Va2	8.5	0.16	1.8	6.1	3.1	0.9	55	15	2.9	5.3	99.62
Va3	14	0.19	3.3	11	1.7	0.8	43	15	5.8	4.1	99.51
Va4	13	0.17	2.9	10	1.5	0.8	44	16	5.5	4.4	99.57

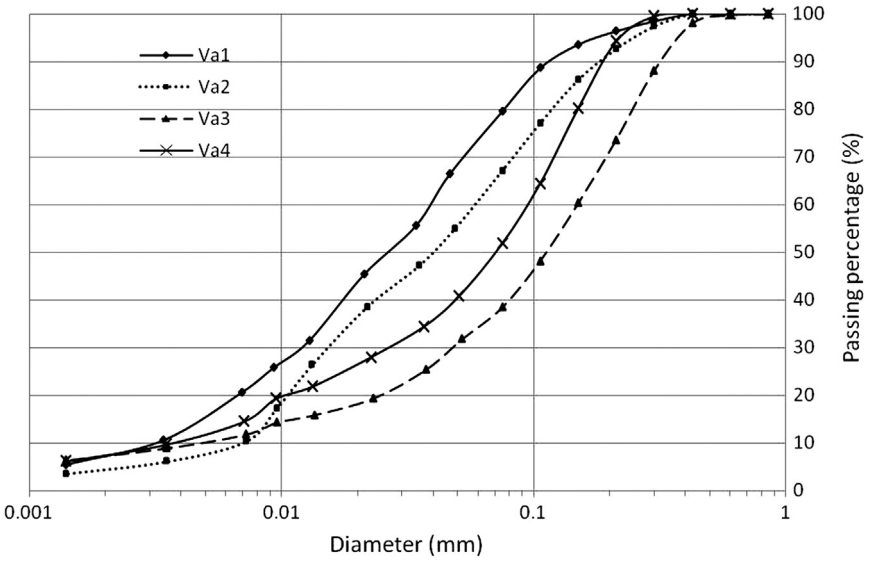

Fig. 1. Particle size distribution of the pure ashes.

Mettler Toledo instrument using Helium at 25 mL/min as a purge gas. The samples were mixed in small quantities (1 g) with a spatula before placing in the sample pan. Reusable high pressure stainless steel sample pans (Mettler) were used. The sample (about 30 mg) was heated from 0 °C to 240 °C at 5 °C/min. For non-isothermal measurements, the sample was heated at 90 °C for 700 min. Temperature calibration was done with cyclohexane and indium. The latter was also used for enthalpy calibration. At least two measurements were performed for each formulation and the error on the reaction enthalpy was below 10%.

2.3. Product characterization

The compressive strength of the samples was measured with an Instron 5885H Compression machine with a displacement of 0.5 mm/min. The results shown here are averages of three replicate specimens. The dry compressive strength was obtained after curing the unmolded products at 90 °C for 5 days. For wet compressive strength, these specimens were immersed in water overnight and measured wet while the wet-dry compressive strength is for immersed specimens dried overnight at 90 °C.

X-ray diffraction was carried out on powdered samples using a D500 Bruker diffractometer, generating a Cu K_α radiation with an applied voltage of 40 kV and a current of 30 mA. XRD scans were measured from 5° to 70° 2-theta at a scan rate of 1°/min.

IR spectra were obtained with a NICOLET 6700 FTIR. For each spectrum, 32 scans with a resolution of 2 cm^{-1} were used in transmission mode on KBr pellets made with 2 mg sample and 200 mg KBr.

EDS maps and scanning electron micrographs of polished samples coated with about 20 nm of carbon for second electron imaging were determined using a Jeol JSM 6400 microscope with an acceleration voltage of 20 kV.

TGA/DTA analyses were performed with a Netzsch STA409 PC/PG instrument in helium flowing at 60 mL/min. The samples were heated to 1000 °C at 10 °C/min.

3. Results and discussion

3.1. Reactivity of the volcanic ashes

The DSC thermograms of the fresh geopolymer mixtures from the different ashes at Na_2O/Al_2O_3 molar ratio of 1.5 are presented in Fig. 2. It is observed that the peak maximum varies between 131 and 166 °C, appearing in the order Va1 < Va3 < Va4 < Va2. The reaction heat of all the fresh geopolymer mixtures from the four ashes with different Na_2O/Al_2O_3 molar ratio (1.00–1.75) are presented in Fig. 3. Globally, it appeared that the reaction heat increases with the amount of NaOH added to the mixture. The trend observed is different from previous studies reported on metakaolin-based geopolymer where the reaction heat was observed to increase with the addition of silicate solution in the fresh mixture, reaching a maximum value at the Na/Al ratio of 1 [11]. This difference could be linked to the mineralogical composition of the ashes, the presence of some crystalline phases dissolving only slowly before reacting, the rate of dissolution increasing with the addition of sodium hydroxide in the mixture. Another reason is that the crystalline reaction product formed (Sodium aluminosilicate hydroxide hydrate-$Na_8(AlSiO_4)_6(OH)_2.4H_2O$) has a Na/Al ratio of 8/6 as shown in previous work [20]. One could thus expect a maximum at a ratio of 1.33 if the amorphous part has the same composition. This however needs further investigation. The temperatures of the maximum reaction rate for all the mixtures are higher while the reaction

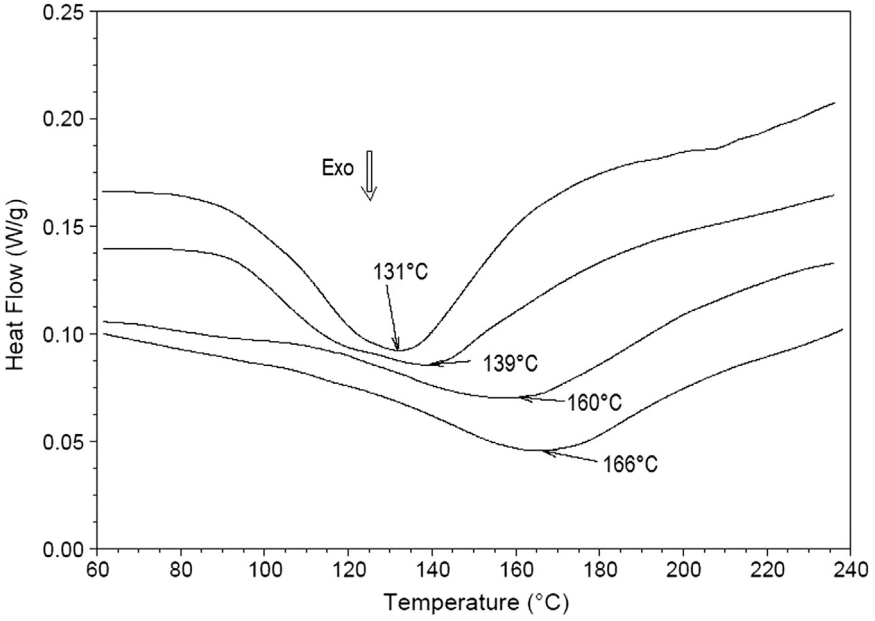

Fig. 2. DSC curves of reacted ashes at Na_2O/Al_2O_3 of 1.50. From the top to the bottom, we respectively have Va1, Va3, Va4 and Va2.

heats are smaller than those reported by Rahier et al. [11,16] for inorganic polymer glasses resulting from alkaline activation of metakaolin, most of the compositions reacting between 60 and 120 °C and the reaction heats reaching 580 J/g metakaolinite. The present volcanic ashes are therefore considered to be less reactive than thermally activated kaolinite. It has been reported that particle size does influence the reactivity, finer particles increasing the reaction rate, the heat flow signal being larger and reaching the baseline earlier [17]. Based on particle size analysis (Fig. 1), the fineness of the ashes were in the range Va1 > Va2 > Va4 > Va3. However, the trend observed on the reaction heats was different ($|\Delta H|$Va1 > $|\Delta H|$Va3 > $|\Delta H|$Va4 > $|\Delta H|$Va2) suggesting that other factors such as the chemical or the mineralogical composition of the ashes were involved. The isothermal measurement at 90 °C of the different ashes (Fig. 4) also showed that the reactivity (height of the signal at the beginning of the measurement) of the ashes are in the order Va1 > Va3 > Va2 > Va4, similarly to the trend observed for the temperatures of appearance of the peak max (Fig. 2) for non-isothermal measurements. As the chemical composition of all the ashes (mostly for Va1, Va3, and Va4) were very similar (Table 1), it is likely that factors that influenced the reactivity should be more linked to the mineralogical composition and crystallinity. Fig. 4 also shows that the main part of the reaction is finished after about 5 h at 90 °C.

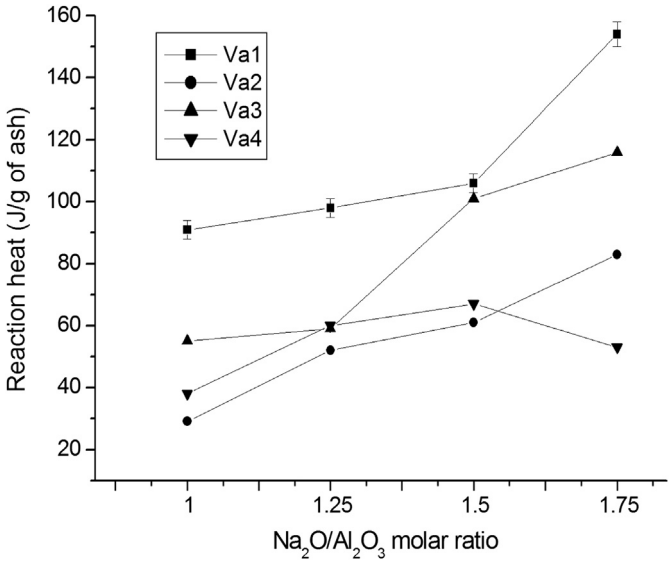

Fig. 3. Reaction heat of freshly mixed mixtures.

3.2. Compressive strength

All the formulations developed strength during the curing period, but still some efflorescence was observable on specimens with high Na content on all the ashes and mostly for Va2 and Va3. The seven days' compressive strengths are presented on Fig. 5. The values of dry compressive strength were between 42 and 61 MPa and 27–63 MPa for products resulting from Va1 and Va2 respectively. For specimens resulting from Va3 and Va4, these values were in the range of 16–32 MPa and 14–37 MPa respectively.

These differences in dry compressive strength noticed between Va1 and Va2 on the one hand and Va3 and Va4 on the other are likely to be linked to the chemical and mineralogical composition of the ashes, but could also be induced by the difference in particle size distribution of the ashes; the ashes with smaller particles (Va1 and Va2) exhibit higher strength than the coarser ones (Va3 and Va4). It was observed that these values decreased after immersion of the samples overnight in water (wet compressive strength) but the strength was partly or totally recovered when the samples were dried overnight at 90 °C. The decrease from the dry to the wet

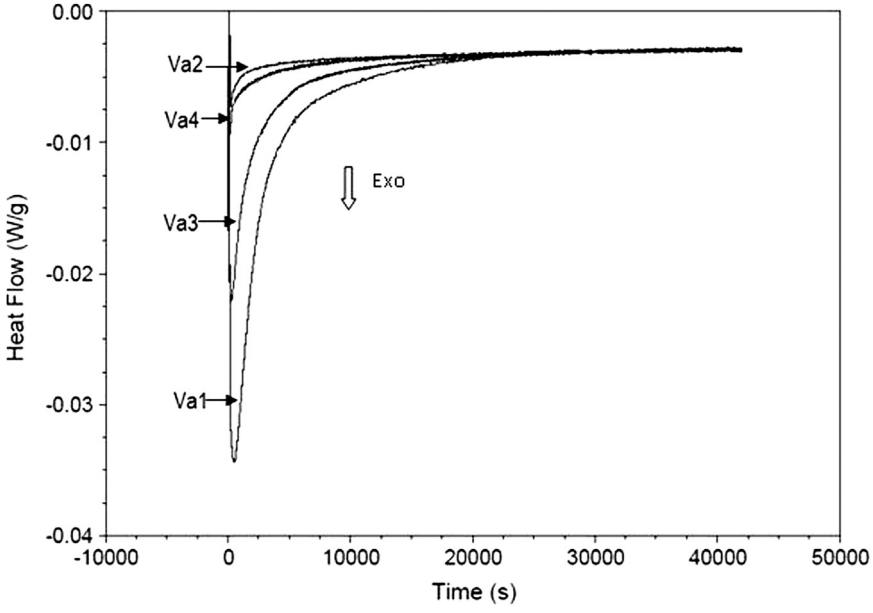

Fig. 4. Isothermal (90 °C) DSC curves of different ashes at Na_2O/Al_2O_3 of 1.50.

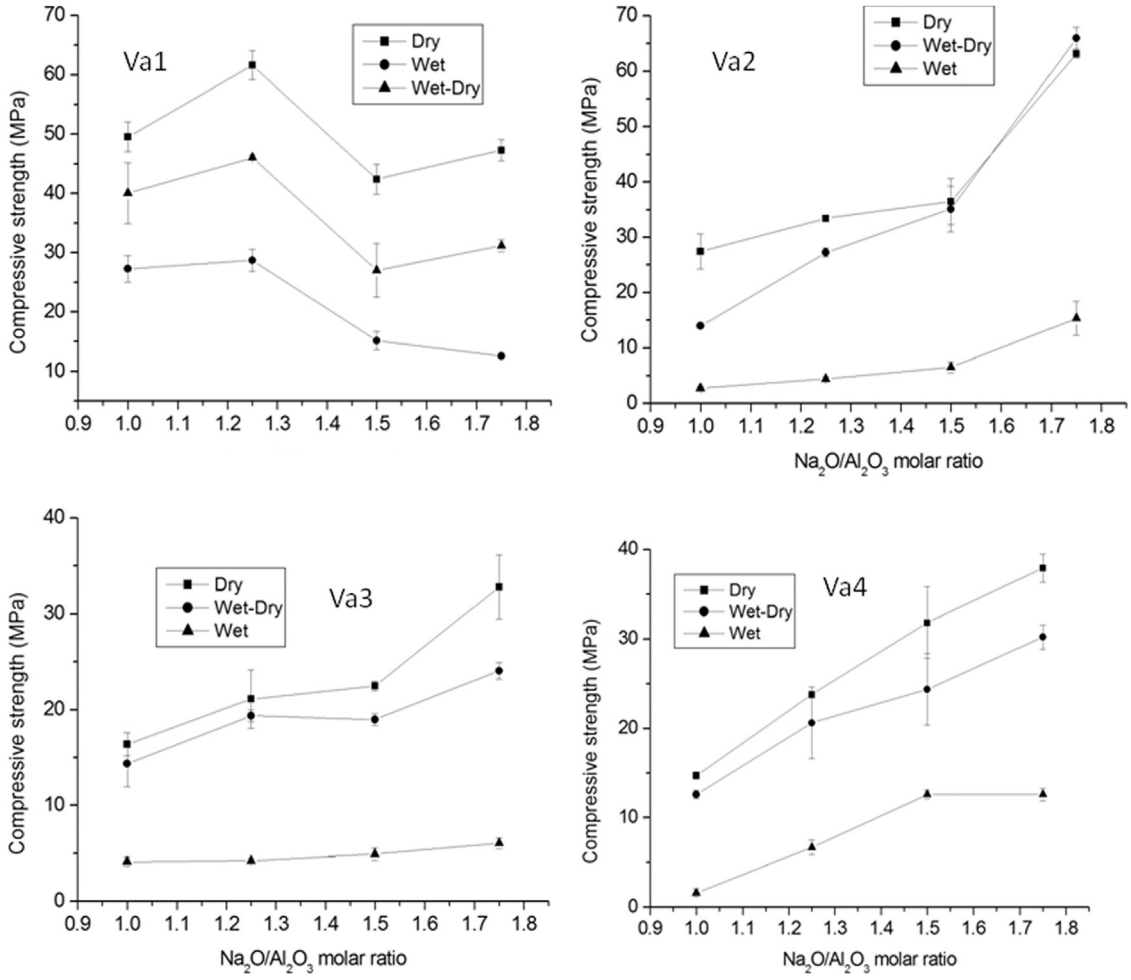

Fig. 5. Compressive strength of reacted ashes.

strength was about 50% for the Va1, but was much more intense for the other samples (about 75% for Va3, moving to 89% for Va2 and Va4 at lowest NaOH concentration). It is well known that this behavior is linked to the hydration of some Si–O–Si bonds to Si–OH bonds in the geopolymer matrix, leading to weakening the structure. This reaction is reversible and was also observed on products resulting from alkali activation of kaolinitic laterite [21]. It is also possible that some soluble components are formed during alkali activation such as sodium silicate, giving a good dry strength but a very low wet strength. Specimens from sample Va1 presented the best wet strengths, with values in the range of 12–28 MPa. The other specimens presented values of wet strength in the range of 1–15 MPa, suggesting their possible higher content in soluble silicate compounds compared with specimens resulting from Va1. After drying, all specimens partially recovered strength. For all the specimens, the wet-dry compressive strengths were in the range 12–65 MPa.

Looking at the chemical composition of the different ashes, it is observed that the ratio Al_2O_3/SiO_2 is between 4.57 and 4.86 for Va1, Va3 and Va4, versus 5.97 for Va2. The optimum value of SiO_2/Al_2O_3 for geopolymer was reported to vary from 3.3 to 4.5 [18], with some possible fluctuation since the amount of Si and Al available for geopolymer formation can be very different depending on the composition and especially the reactivity of the starting raw materials [19]. Considering the lower reaction heat and lower reactivity (the highest temperature of peak max on the DSC curves Fig. 2) observed for sample Va2, it is likely that this sample presented some excess of reactive SiO_2.

Increasing the amount of NaOH to the system leads to increasing the final strength up to a maximum value of 61 MPa with a ratio Na_2O/Al_2O_3 of 1.25 for Va1, following the trend observed in previous report on metakaolin and volcanic ashes based geopolymer [20,22]. It was also observed on the specimens resulting from this particular ash (Va1) that excess NaOH leads to crack formation on the specimens, the size of cracks increasing with NaOH addition. Such an optimum (the decrease of compressive strength beyond some amount of NaOH used) is not observed for the other ashes that show an increase of the strength with added NaOH in the range of our study (Na_2O/Al_2O_3 of 1.00–1.75), although the excess of unreacted NaOH was obvious from the white efflorescence (Na_2CO_3) visible on samples resulting from Na_2O/Al_2O_3 of 1.75.

The difference observed while adding NaOH into the system of the present ashes could be linked to the type and amount of crystalline phases over the amorphous phase in the starting materials as will be done in the next part. For Va1, we have

more reactive amorphous phase that dissolves quickly in alkaline medium; the effect of excess NaOH on the strength reduction being observable from Na_2O/Al_2O_3 of 1.50 on. That is different for the other ashes where we have a smaller amorphous fraction, and where increasing the NaOH content probably also has as major effect on the dissolution of the amount of crystalline phases, increasing the amount of reacting materials and the final strength. Therefore, the higher value of dry strength observed for Va2 is much more linked to its mineralogical composition since the reaction heat remains very low.

3.3. Mineralogical composition of volcanic ashes and geopolymers

The X-ray spectra of the volcanic ashes show a mixture of amorphous and crystalline phases (Fig. 6) composed of Anorthite sodian disordered:$(Ca,Na)(Si,Al)_4O_8$, Augite: $(CaMg_{0.74}Fe_{0.25})Si_2O_6$, Forsterite ferroan: $(Mg_{0.9}Fe_{0.1})_2SiO_4$ for Va1; Quartz: SiO_2 Augite: $(CaMg_{0.74}Fe_{0.25})Si_2O_6$, Magnetite: Fe_3O_4, Anorthite sodian intermediate-$(CaNa)(SiAl)_4O_8$, Microline intermediate-$KAlSi_3O_8$ for Va2; Anorthite sodian disordered: $(Ca,Na)(Si,Al)_4O_8$, Augite: $(CaMg_{0.74}Fe_{0.25})Si_2O_6$, Forsterite ferroan: $(Mg_{0.9}Fe_{0.1})_2SiO_4$ for Va3 and Anorthite sodian disordered: $(Ca,Na)(Si,Al)_4O_8$, Augite: $(CaMg_{0.74}Fe_{0.25})Si_2O_6$, Nepheline: $NaAlSiO_4$, Forsterite: Mg_2SiO_4, Hematite: Fe_2O_3 for Va4. The main difference observable by XRD between the spectra of pure ashes and those treated with sodium hydroxide were the appearance of sodium aluminosilicate hydroxide hydrate $Na_8(AlSiO_4)_6(OH)_2.4H_2O$ on the spectra of activated ashes. The presence of initial minerals in the final products is also suggesting incomplete dissolution of the crystalline phases present in the starting materials. Conventional geopolymers resulting from the dissolution of aluminosilicate in a strongly alkaline medium are expected to be amorphous [9,11,23]. However, the presence of a new crystalline phase not originating from the starting material has been previously reported for geopolymers resulting from volcanic ash, fly ash as well as metakaolinite especially after reaction with silicates with a low modulus [4,16,20,24].

By treating an amorphous pozzolan with sodium hydroxide or sodium hydroxide plus sodium aluminate, Verdolotti et al. [4] obtained a product with crystalline diffraction peaks, possibly from a zeolite, overlapping the amorphous baseline. For the current volcanic ashes, it is likely that the reactions that took place in alkaline medium may involve the transformation of the major part of the initial amorphous phases of the ash into the amorphous to semi crystalline geopolymer phase, but also a crystalline phase of sodium aluminosilicate hydroxide hydrate. The formation of this new crystalline phase (sodium aluminosilicate hydroxide hydrate, sometime named as hydroxysodalite) during inorganic polymers synthesis was suggested to be linked to the nature of the initial starting material, the

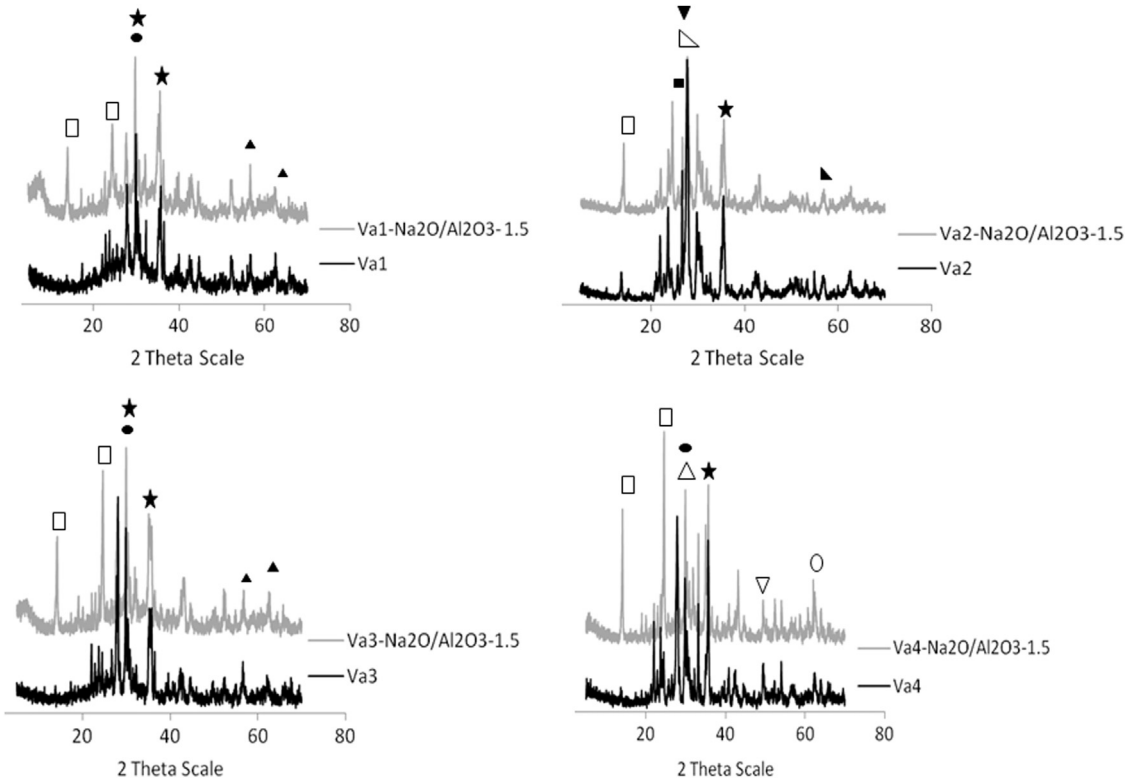

Fig. 6. XRD spectra of pure (bottom) and reacted ashes at Na_2O/Al_2O_3 of 1.50. •=Anorthite sodian disordered:$(Ca,Na)(Si,Al)_4O_8$,. ★=Augite: $(CaMg_{0.74}Fe_{0.25})Si_2O_6$, ▲=Forsterite ferroan: $(Mg_{0.9}Fe_{0.1})_2SiO_4$, ■=Quartz: SiO_2. ◣=Magnetite: Fe_3O_4, ▼=Microline intermediate-$KAlSi_3O_8$, ◺=Anorthite sodian intermediate-$(CaNa)(SiAl)_4O_8$. ○=Forsterite: Mg_2SiO_4. Δ=Nepheline:$NaAlSiO_4$, ∇=Hematite: Fe_2O_3. □=sodium aluminosilicate hydroxide hydrate-$Na_8(AlSiO_4)_6(OH)_2 \cdot 4H_2O$.

curing temperature and the concentration/composition of the alkaline solution used [25,26]. Finally, the alteration or transformation of part of the initial crystalline phase in the starting ashes is also likely to have taken place during alkali activation.

The amount of amorphous phase was estimated with the analysis software by the method of subtracting the crystalline surface area on the XRD spectra. The results obtained were 58% for Va1, 6% for Va2, 33% for Va3 and 9% for Va4. After reaction, the amount of amorphous phase in the products was estimated at a Na_2O/Al_2O_3 molar ratio of 1.50 to be 44%, 27%, 37% and 29% respectively in the specimens resulting from Va1, Va2, Va3, and Va4. A positive correlation was found between the amount of the amorphous phase in the ash and the heats of reaction (Fig. 7). The determination of the linear correlation equation gave $y=1.12x+23.68$, with a linear correlation coefficient of 0.97.

This trend was also observable on the DSC curves (Figs. 2 and 4) showing higher reaction heat and reactivity for the more amorphous materials. An extrapolation of the curve (Fig. 7) shows that there is still some reactivity remaining at 0% of amorphous material, suggesting that small part of the crystalline phases also reacted. This can explain the increase of the amount of amorphous fraction after reaction for Va2, Va3 and Va4. The trend observed on the values of wet strength at lowest NaOH concentration are in line with the amount of amorphous phase in the starting materials and the sample that globally presented the best strengths also resulted from the more amorphous starting material (Va1). For the higher concentrations of sodium hydroxide the correlation between the amount of amorphous phase in the starting materials and the final strength after 7 days curing is less obvious.

In summary, one can state that Va1 ash has the largest amount of amorphous reactive phase dissolving quickly giving the largest reaction heat and best compressive strength. The effect of excess NaOH on the strength reduction is observable from Na_2O/Al_2O_3 of 1.50 on. This could be explained by the fact that the crystalline component found after reaction has a Na/Al ratio of 1.33, which could be considered as the maximum and thus optimum ratio. All other ashes have a much smaller amorphous fraction, and increasing the NaOH content probably also increases the amount of crystalline phases dissolved, increasing the amount of reacting materials and thus the reaction heat and the final strength. It is however supposed that an excess of NaOH is needed to dissolve the crystals. Therefore, the relatively high value of dry strength observed for Va2 is probably more linked to its mineralogical composition since the reaction heat remains very low. The fact that the wet strength is very low indicates the formation of soluble reaction products.

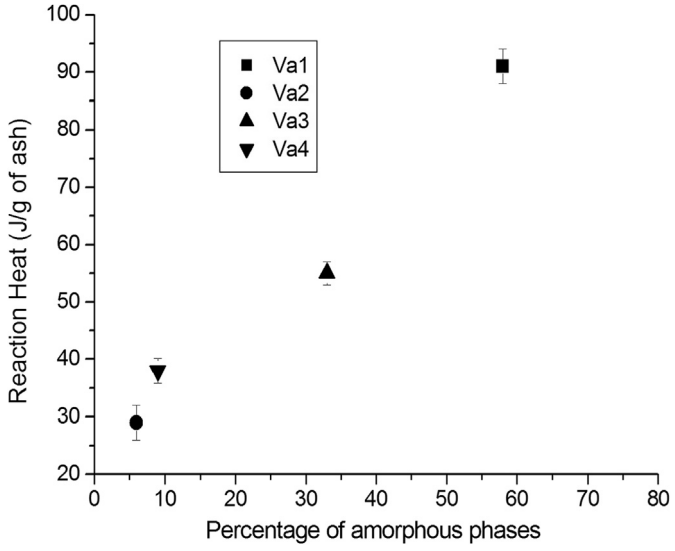

Fig. 7. Influence of the percentage of the amorphous phase in the starting ashes on the reaction heat at Na_2O/Al_2O_3 molar ratio of 1.00.

3.4. IR spectra

The infrared spectra presented in Fig. 8 showed a broad absorbance at 820–1250 $cm^{-1}$and 480–600 cm^{-1} assigned to internal vibration of Si–O–Si and Si–O–Al [20,27] in both raw volcanic ash and resulting inorganic polymer samples. The appearance of some sharp bands indicates the formation of crystalline phases. The band around 1640 cm^{-1} arises from water molecules, which are surface absorbed or entrapped in the large cavities of the polymeric framework. This band which

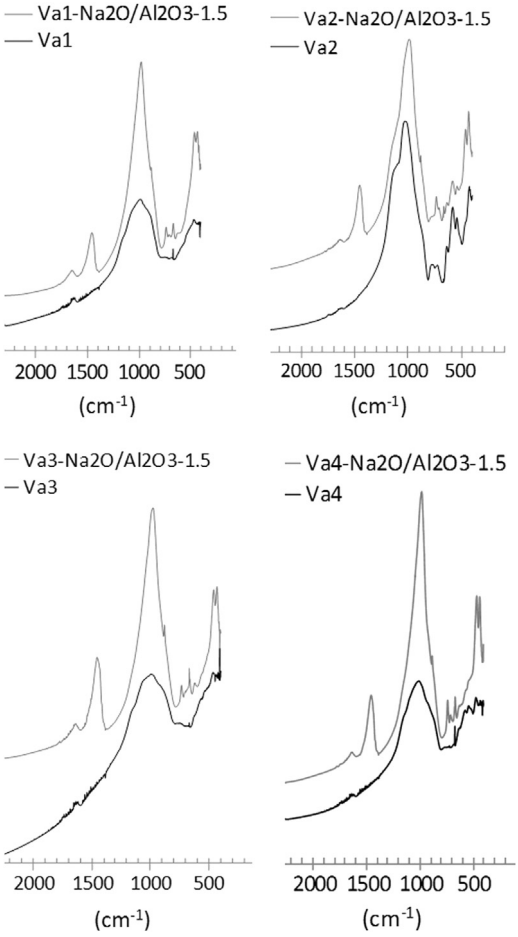

Fig. 8. IR spectra of pure (bottom) and reacted ashes at Na_2O/Al_2O_3 of 1.50.

was mostly observed on alkali-activated ashes is attributed to bending vibrations (H–O–H) and is typical for polymer structures including aluminosilicate networks [25,26]. The band around 1430 cm^{-1} on the alkali-activated ashes is attributed to stretching vibrations of the O–C–O bond resulting from the atmospheric carbonation of the unreacted high alkaline aqueous phase, which is diffused on the geopolymeric materials surface [20,24]. The relatively strong peaks seen at ~1002 cm^{-1} (as well as at ~458 cm^{-1}) on the alkali-activated ashes are assigned to long chain bonds and/or the excess of Al–Si gel formed [25].

3.5. Microstructure

The microstructural analysis of polished products shows that the particle dissolution is not completed during the reaction (Fig. 9A). Relicts of ash particles were found to be surrounded by the geopolymer matrix. The morphologies of all the samples were similar at lower magnification. However, higher magnification (Fig. 9B) presented a mixture of late shaped and agglomerate morphology with a great tendency for agglomeration for Va2 and Va4, possibly suggesting a more crystalline character. Geopolymers are known to contain amounts of unreacted solid aluminosilicate source [28,29]. However, there is no definitive and accurate method for quantitatively determining the amount of unreacted materials in a particular specimen. The unreacted material is also expected to affect the mechanical properties [28].

The geopolymer matrix was the only part of the sample to contain added sodium, and was found by EDS in the area selected to correspond to the atomic composition of Al_5 at%, Si_13 at%, Na_13 at% for Va1; Al_3 at%, Si_25 at%, Na_8 at% for Va2; Al_5 at%, Si_15 at%, Na_25 at% for Va3;

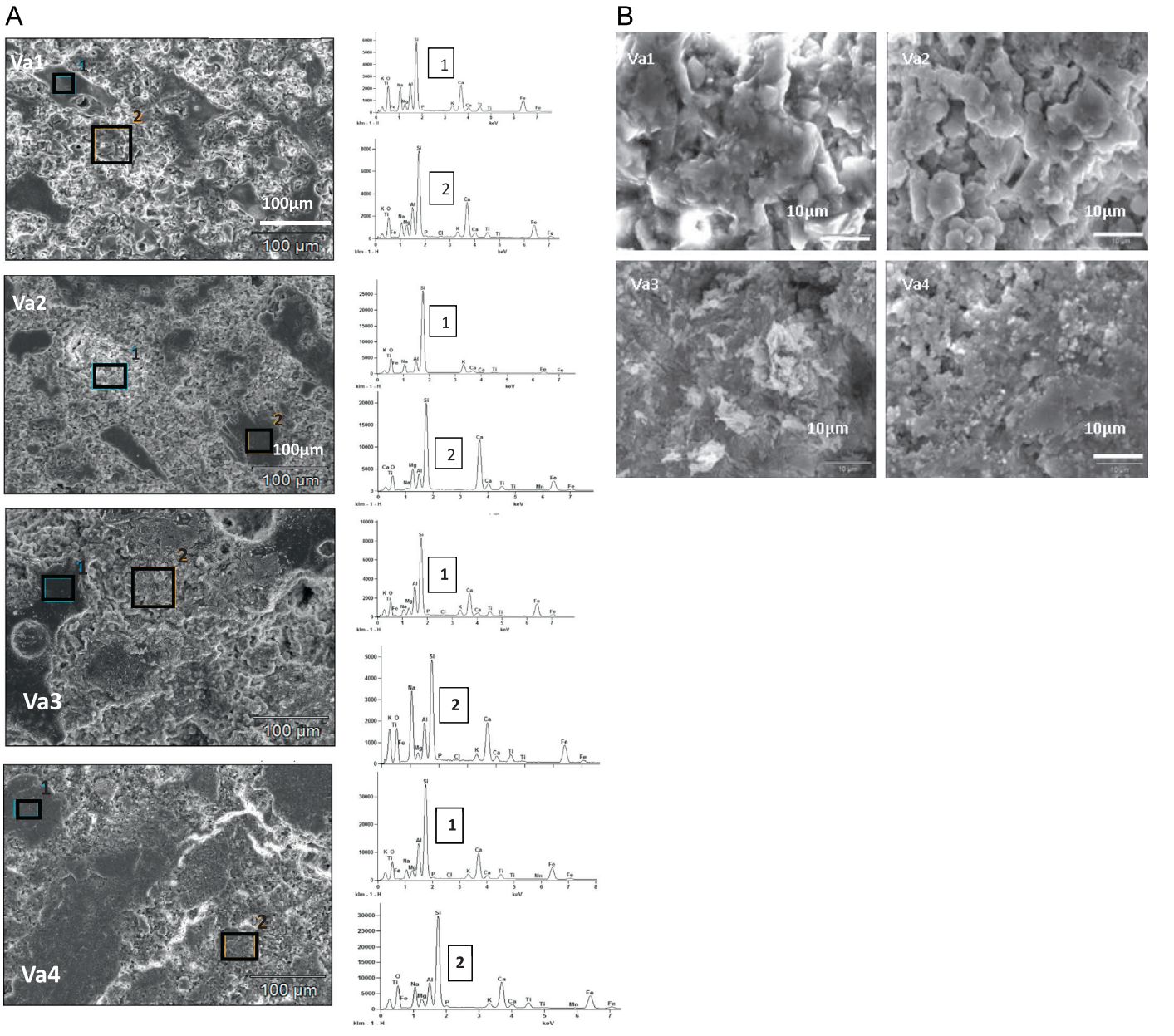

Fig. 9. Microstructure of reacted ashes at Na_2O/Al_2O_3 of 1.50.

Al_5 at%, Si_18 at%, Na_12 at% for Va4. It is striking that these compositions do not match the composition of the formed sodium aluminosilicate $Na_8(AlSiO_4)_6(OH)_2 \cdot 4H_2O$. The high atomic concentration of sodium in the geopolymer matrix on the area selected for the geopolymer based on Va3 could arise from its migration due to atmospheric condition. The fluctuations observed in the geopolymer matrix compositions may be due to the presence of some small residual undissolved particles with different chemical composition. It is also likely that some divergence in the geopolymer matrix composition from the different ashes could be linked to the difference in the proportion of sodium aluminosilicate hydroxide hydrate formed and mixed with the amorphous part of the matrix.

3.6. Thermal behavior (TG/DTA)

The thermal behavior of synthesized products assessed by thermogravimetry analysis and differential thermal analysis are presented in Fig. 10. The pure ashes show almost no weight loss up to 1000 °C (less than 1 wt%) (Fig. 10A). Globally, the DTA and the TGA curves are more or less similar for all the samples. It is observed that the mass losses are between 3.5 and 6%. Sample Va2 presented the lowest mass loss (around 3.5%), possibly in consistence with its small reactivity observed in the DSC analysis, those of the other ashes being between 5.5 and 6% (Fig. 10B). On the DTA curves, the endothermic reaction observed below 200 °C is attributed to the loss of residual water after the curing period. Above this temperature, no clear endothermic reaction is observed up to 1000 °C. After 200 °C, all the samples were found to lose mass at a more or less constant rate up to 600 °C, above which the mass loss becomes negligible up to 1000 °C. Between 200 °C and 600 °C, the mass loss is likely to arise from the destruction of some structured OH in the products matrix since the loss on ignition was negligible for all the pure ashes. The mass loss of all the synthesized specimens are about four times smaller than those reported (about 25%) for metakaolin based geopolymer [23,30] after heating up to 1000 °C. However, these products were already dried in the furnace at 90 °C during the curing while the products from metakaolin resulted from a curing at 50 °C [23] or at room temperature [30].

4. Conclusions

The four ashes subjected to analysis were found to have great similarities in chemical compositions and the parameter which greatly influenced the reactivity was found to be the amount of amorphous fraction. The reactivity and the reaction heat of the systems increases with the amount of these amorphous phases in the starting ashes. The compressive strength was found to decrease after immersion of the specimens overnight in water, but was partly or totally recovered after overnight drying at 90 °C. The dry compressive strengths of synthesized products from all the ashes were in the range

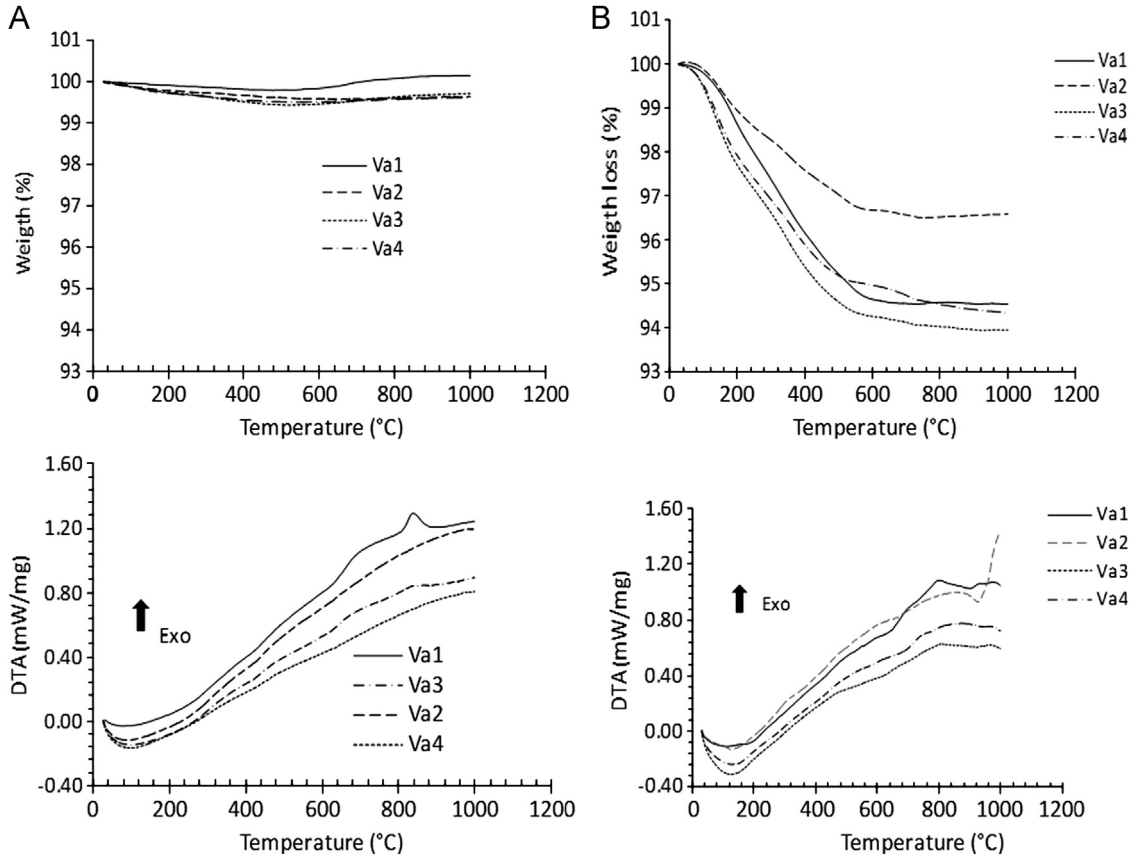

Fig. 10. TG/DTA curves of pure (A) and reacted (B) ashes at Na_2O/Al_2O_3 of 1.50.

14–63 MPa suggesting their possible utilization as building materials.

Specimens from the most amorphous sample Va1 presented the best wet strengths, with values in the range of 12–28 MPa. The other specimens presented values of wet strength in the range of 1–15 MPa. For all the specimens, the wet-dry compressive strengths were in the range 12–65 MPa. The wet strength at lowest NaOH concentration also increases with the amount of amorphous phase in the volcanic ashes and the sample that globally presented the best strengths also resulted from the more amorphous starting material (Va1). When high NaOH concentrations were used, no correlation between the amount of amorphous phase in the starting materials and the final strength could be established.

The suitability of volcanic ashes for geopolymerization thus does not only depend on the chemical composition but also on the fraction of amorphous material. Further investigations on different types of activating solution and the durability of the materials for building applications will be of interest.

Acknowledgments

The authors would like to thank T. Segato for assistance with the X-ray diffraction and the VLIR-UOS-SRS-intake 2011 program which supported the stay of PNL at VUB.

References

[1] J. Davidovits, Geopolymers: man-made rock geosynthesis and the resulting development of very early high strength cement, Materials Education 16 (1994) 91–139.
[2] C. Leonelli, E. Kamseu, D.N. Boccaccini, U.C. Melo, A. Rizzuti, N. Billong, P. Misselli, Volcanic ash as alternative raw materials for traditional vitrified ceramic products, Advances in Applied Ceramics 106 (2007) 1.
[3] P. Ntep Gweth, J.J. Dupuy, O. Matip, A. Fombutu Fogakoh, E. Kalngui, Ressources Minérales du Cameroun, Ministère des Mines, de l'Eau et de l'Energie, Yaoundé, Juillet 2001.
[4] L. Verdolotti, S. Iannace, M. Lavorgna, R. Lamanna, Geopolymerization reaction to consolidate incoherent pozzolanic soil, Journal of Materials Science 43 (2008) 865–873.
[5] D. Bondar, C.J. Lynsdale, N.B. Milestone, N. Hassani, A. A. Ramezanianpour, Effect of type, form, and dosage of activators on strength of alkali-activated natural pozzolans, Cement and Concrete Composites 33 (2011) 251–260.
[6] H. Rahier, B. Wullaert, B. Van Mele, Influence of the degree of dehydroxylation of kaolinite on the properties of aluminosilicate glasses, Journal of Thermal Analysis and Calorimetry 62 (2000) 417–427.
[7] H. Rahier, J. Wastiels, M. Biesemans, R. Willlem, G. Van Assche., B. Van Mele, Reaction mechanism, kinetics and high temperature transformations of geopolymers, Journal of Materials Science 42 (2007) 2982–2996.
[8] H. Nugteren, Secondary Industrial Minerals From Coal Fly Ash and Aluminium Anodising Waste Solutions, Ph.D thesis, TuDeft University of Technology, Netherland, 2010.
[9] V.F.F. Barbosa, K.J.D. MacKenzie, C. Thaumaturgo, Synthesis and characterisation of materials based on inorganic polymers of alumina and silica: sodium polysialate polymers, Inter, Journal of Inorganic Materials 2 (2000) 309–317.
[10] E. Obonyo, E. Kamseu, U.C. Melo, C. Leonelli, Advancing the use of secondary inputs in geopolymer binders for sustainable cementitious composites: a review, Sustainability 3 (2011) 410–423.
[11] H. Rahier, B. Van Mele, M. Biesemans, J Wastiels., X Wu, Low-temperature synthesized aluminosilicate glasses. Part I. Low-temperature stoichiometry and structure of a model compound, Journal of Materials Science 31 (1996) 71–79.
[12] H. Ruscher Claus, M. Mielcarek Elzbieta, J. Wongpa, C. Jaturapitakkul, F. Jirasit, L. Lohaus, Silicate–aluminosilicate and calciumsilicate gels for building materials: chemical and mechanical properties during ageing, European Journal of Mineralogy 23 (2011) 111–124.
[13] P. Duxson, G.C. Lukey, J.S.J. van Deventer, Thermal evolution of metakaolin geopolymers: Part 1. Physical evolution, Journal of Non-Crystalline Solids 352 (2006) 5541–5555.
[14] C. Shi, A. Fernández Jiménez, A. Palomo, New cements for the 21st century: the pursuit of an alternative to Portland cement, Cement and Concrete Research 41 (2011) 750–763.
[15] P. Duxson, J.L Provis, G.C Lukey, J.S.J van Deventer, The role of inorganic polymer technology in the development of 'green concrete', Cement and Concrete Research 37 (2007) 1590–1597.
[16] H. Rahier, W. Simon, B. Van Mele, M. Biesemans, Low-temperature synthesized aluminosilicate glasses. Part III. Influence of the composition of the silicate solution on production, structure and properties, Journal of Materials Science 32 (1997) 2237–2247.
[17] H. Rahier, F.J. Denayer, B. Van Mele, Low-temperature synthesized aluminosilicate glasses part IV modulated dsc study on the effect of particle size of metakaolinite on the production of inorganic polymer glasses, Journal of Materials Science 38 (2003) 3131–3136.
[18] K. Komnitsas, D. Zaharaki, Geopolymereisation: a review and prospects for minerals industry, Minerals Engineering 20 (2007) 1261–1277.
[19] P. De Silva, K. Sagoe-Crenstil, V. Sirivivatnanon, Kinetics of geopolymerization: role of Al_2O_3 and SiO_2, Cement and Concrete Research 37 (2007) 512–518.
[20] P.N. Lemougna, K.J.D MacKenzie, U.F.C. Melo, Synthesis and thermal properties of inorganic polymers (geopolymers) for structural and refractory applications from volcanic ash, Ceramics International 37 (2011) 3011–3018.
[21] C. Boutterin, J. Davidovits, Réticulation Géopolymérique (LTGS) et Matériaux de Construction, Géopolymère 1 (2003) 79–88.
[22] C.H. Rüscher, E. Mielcarek, W. Lutz, A. Ritzmann, W.M. Kriven, Weakening of alkali-activated metakaolin during aging investigated by the molybdate method and infrared absorption spectroscopy, Journal of the American Ceramic Society 93 (2010) 2585–2590.
[23] J.L. Bell, P.E. Driemeyer, W.M Kriven, Formation of ceramics from metakaolin-based geopolymers: Part II. K-based geopolymer, Journal of the American Ceramic Society 92 (2009) 607–615.
[24] D. Panias, P. Ioanna. Giannopoulou, T. Perraki, Effect of synthesis parameters on the mechanical properties of fly ash-based geopolymers, Colloids and Surfaces A: Physicochemical and Engineering Aspects 301 (2007) 246–254.
[25] D. Zaharaki, K. Komnitsas, V. Perdikatsis, Use of analytical techniques for identification of inorganic polymer gel composition, Journal of Materials Science 45 (2010) 2715–2724.
[26] K. Komnitsas, D. Zaharaki, V. Perdikatsis, Effect of synthesis parameters on the compressive strength of low-calcium ferronickel slag inorganic polymers, Journal of Hazardous Materials 161 (2009) 760–768.
[27] J. Davidovits, Geopolymer Chemistry and Application, 2nd edition, Institut Géopolymère, Saint-Quentin, France, 2008.
[28] P. Duxson, J.L. Provis, G.C. Lukey, S.W. Mallicoat, W.M. Kriven, J.S. J. van Deventer, Understanding the relationship between geopolymer composition, microstructure and mechanical properties, Colloids and Surfaces A: Physicochemical and Engineering Aspects 269 (2005) 47–58.
[29] M. Schmückera, K.J.D. MacKenzie, Microstructure of sodium polysialate siloxo geopolymer, Ceramics International 31 (2005) 433–437.
[30] H. Rahier., B. Van Mele, J. Wastiels, Low-temperature synthesized aluminosilicate glasses. Part II Rheological transformations during low-temperature cure and high-temperature properties of a model compound, Journal of Materials Science 31 (1996) 80–85.